THE MICROSCOPE • Vol 58:2, pp 51-62 (2010)

Asbestos Fiber Counting by Different Optical Contrast Techniques

Anthony A. Havics
pH2, LLC*

KEYWORDS

Asbestos, amosite, chrysotile, man-made mineral fibers (MMMF), fiber counting, Phase contrast microscopy (PCM), Hoffman Modulation Contrast (HMC), Nomarski differential interference contrast (DIC)

ABSTRACT

Fiber counting of asbestos using light microscopy has traditionally been performed using phase contrast microscopy (PCM) techniques. The use of phase contrast for counting has several weaknesses, including difficulties with fiber detection and overlapping diffraction patterns causing the appearance of "false" fibers or masking fibers. It is, however, a significant improvement over ordinary brightfield microscopy. The purpose of this study was to assess the use of two other contrast techniques, Hoffman modulation contrast (HMC) and Nomarski differential interference contrast (DIC). Samples of three fiber types, chrysotile, amosite, and man-made mineral fibers (MMMF) were used for this evaluation. DIC faired poorly in general and HMC faired reasonably well. The differences can be explained by the general aspects of contrast production in reference to phase detection and imaging of each method.

INTRODUCTION

Fiber counting of asbestos using the light microscope has traditionally been performed using phase contrast microscopy (PCM) techniques (1-5). The purpose of using phase contrast as opposed to ordinary light microscopy is the additional contrast, and therefore the *de facto* resolution or opportunity to detect fibers. This study was carried out to evaluate two other techniques to enhance visibility of fibers, namely Hoffmann modulation contrast (HMC) and Nomarski differential interference contrast (DIC), both of which are also "contrast enhancement" techniques.

MICROSCOPY TECHNIQUES UTILIZED

The three microscopy techniques of PCM, HMC and DIC use increased contrast to enhance visibility. PCM was introduced by Frits Zernike in 1934 (6, 7). PCM uses a phase shifting element in combination with proper illumination through a phase annulus and specimen light-wave deviation to create contrast. As shown in Figure 1 illustrating PCM, the light is restricted to a narrowed (usually) annular pathway in the substage condenser. The light then is directed to the specimen where it is acted upon by the specimen causing a phase deviation on the order of one-quarter of a wavelength [(1/4)λ] between direct and indirect light waves. The light is then collected and directed by the objective lenses through the back focal plane where a phase ring is situated. The size of the annular opening matches the size of the phase ring in the back focal plane of the phase objective. Here, the direct and indirect light waves are further separated by another (1/4)λ shift as the one passes through the phase ring. Upon recombining, the direct and indirect

*5250 E. U.S. Hwy. 36, Suite 830, Avon, IN 46123

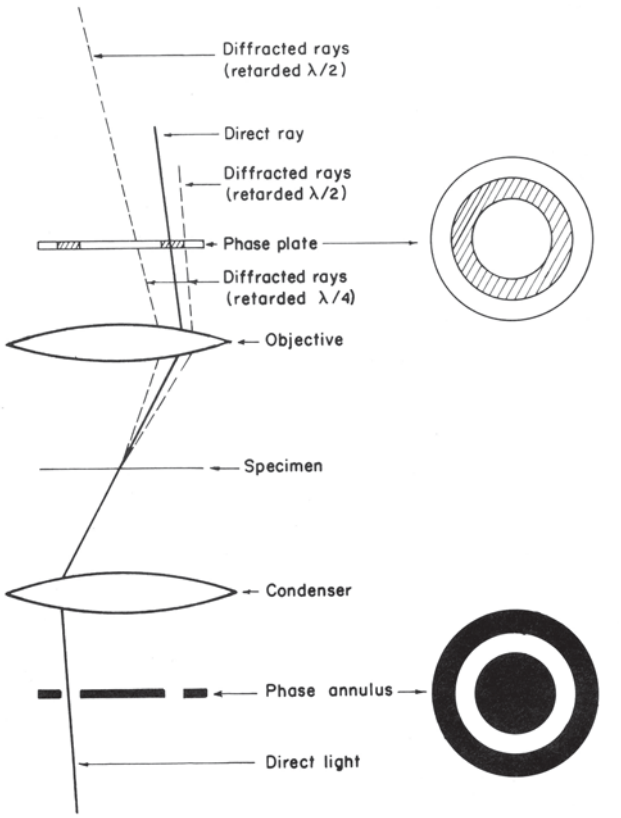

From *Polarized Light Microscopy* (McRI, 1984)

Figure 1. Phase Contrast Microscopy (PCM) showing exaggerated paths of direct and indirect light waves.

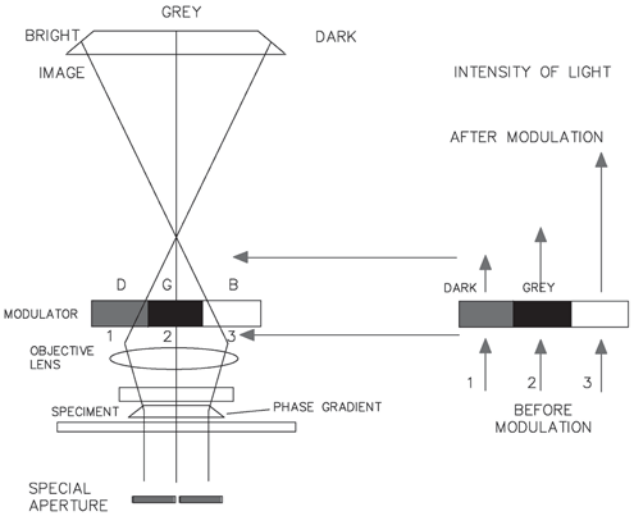

Courtesy of Dr. Robert Hoffman

Figure 2A. Components and light paths of Hoffman Modulation Contrast (HMC).

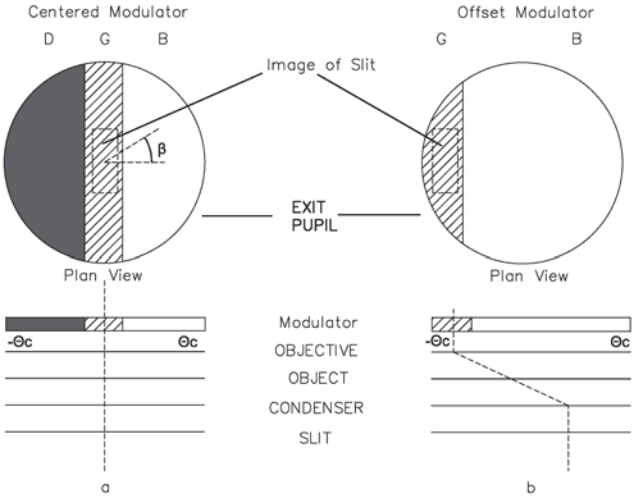

Courtesy of Dr. Robert Hoffman

Figure 2B. HMC transmission characteristics reveal the effect of accentuating differences in contrast by superposition.

light waves are approximately (1/2)λ out of phase, resulting in destructive interference that cancels out both waves and consequently creates a dark (black) image of the specimen. In the case of asbestos, a thin fibrous structure is revealed. For total deviation differences of nλ/2 [n= 1, 2, 3...] darkness will be displayed, and for total deviation differences of nλ [n= 0, 1, 2, 3...] brightness will be displayed.

The technique of HMC, first invented by Robert Hoffman (8, 9), involves using an off-axis slit placed in front of the focal plane of the condenser (Figure 2A). This effectively illuminates the specimen with oblique illumination. At the back of the focal plane of the objective there is a plate (the Hoffman modulator) with three different size neutral-density regions — transparent (100% light transmission), gray (15% transmission) and dark gray (1% transmission). This is placed so that the slit aperture is aligned with the 15% transmission region. When light passes through various regions of the sample, light is refracted to different degrees passing either through the transparent, gray or dark gray regions of the modulator. This has the effect of accentuating differences in contrast by superposition (Figure 2B).

Polarizing filters may also be used in Hoffman modulation contrast systems to further enhance contrast. Images may appear similar to those obtained in Nomarski DIC imaging. Unlike DIC, however, Hoffman Modulation Contrast does not use beam-splitting prisms. It can also be used with specimens not suitable for DIC (crystalline substances or living specimens

in plastic culture dishes). Hoffman modulation contrast imaging also avoids halos that are sometimes observed in phase contrast imaging. Modulation contrast was not invented by Hoffman but he refined it in a specific way (10). In addition, the contrast is directional relative to the gradient.

Nomarski DIC was invented by Georges Nomarski in the mid 1950s (11). It is used to image specimens that contain little or no optical contrast when viewed using ordinary brightfield illumination. In transmitted light DIC (used in this study), light passes through a polarizer located beneath the condenser in a manner similar to polarized light microscopy (PLM), therefore becoming plane polarized light. The polarized light then passes though a Wollaston prism located in the front focal plane of the condenser (Figure 3). The prism splits the beam of light into two beams traveling in slightly different directions but vibrating at 90 degrees to each other. Because they are perpendicular they are unable to recombine (and cause interference).

The distance between the two beams is called the "shear" distance and is always less than the resolving ability of the objective to prevent the appearance of double images. The split beams enter and pass through the specimen. At this point their paths are altered by the specimen's varying thickness, geometry and refractive index(es). When the parallel beams enter the objective, they are focused above the back focal plane where they enter a second modified Wollaston prism that recombines the two beams at a defined distance outside of the prism. This removes the shear and the original path difference between the beam pairs. However, the parallel beams are no longer the same length because of path changes induced by passing through the specimen.

In order for the parallel beams to interfere with each other, the vibrations of the beams of different path length must be brought into the same plane and axis. This is accomplished by placing a second polarizer (analyzer) above the upper modified Wollaston beam-combining prism. The light then proceeds toward the eyepiece where it can be observed as differences in intensity and color. DIC microscopy causes one side of an object to appear bright (or colored) while the other side appears dark (or a different color). This shadow effect gives a pseudo three-dimensional appearance to the specimen, but it is not a true representation of the geometry of the specimen because it is based on optical thickness not just physical thickness. The pseudo-3D appearance of the specimen can also be significantly affected by its orientation, that is, the rotation of the specimen by 180 degrees can change a convex surface into a concave one.

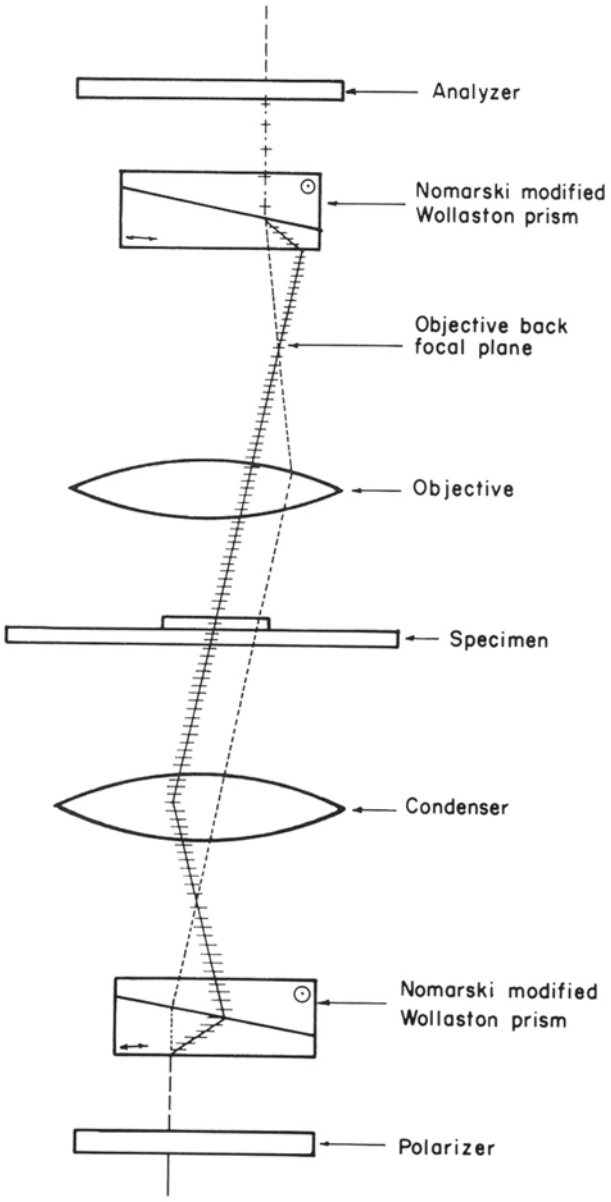

From *Polarized Light Microscopy* (McRI, 1984)

Figure 3. Nomarski Differential Interference Contrast (DIC) Microscopy showing exaggerated paths of light waves.

These are some advantages in DIC microscopy as compared particularly to phase microscopy. Using DIC microscopy, it is possible to make more use of the numerical aperture of the system because, unlike phase contrast microscopy, there is no substage annulus to restrict the aperture, therefore, Köhler illumination is properly achieved. Images can be seen in striking color (optical contrast) with a three-dimensional shadow-

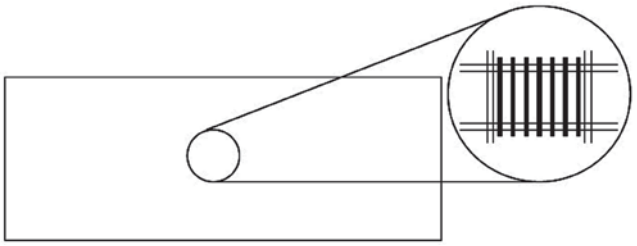

Figure 4. HSE/NPL Test Side with seven sets of approximately 20 grooves per set in descended order of width and visibility from 1.08 µm to 0.25 µm. Set 3 (0.64 µm) must be completely resolved and parts of sets 4 and 5 (0.53-0.44 µm) must be visible.

like appearance. DIC does not produce halos like those encountered in phase images. There are, however, several disadvantages in DIC microscopy; the equipment for DIC is quite expensive due to the many prisms that are required. Birefringent specimens, such as those found in many kinds of crystals, may not be suitable because of their effect upon polarized light. Similarly, specimen carriers made of plastic, such as culture vessels, Petri dishes, etc., may not be suitable. For very thin or scattered specimens, better images may be achieved using phase contrast methods, as was seen in this study with thin chrysotile fibers.

EXPERIMENTAL DESIGN PART 1: SAMPLES AND EQUIPMENT

A total of 18 samples from the National Institute for Occupational Safety & Health (NIOSH) Precision Analytical Testing (PAT) with known reference values from more than 1,200 laboratories were utilized (3, 12-14). Six samples, each from three types of fibers were selected for analysis. These types were amosite asbestos, chrysotile asbestos and man-made mineral fibers (MMMF). Samples consist of 0.8 mm pore-size mixed cellulose ester (MCE) filters mounted in 25 mm diameter cassettes. On (and in) the filters are fibers presumed to be randomly oriented in the plane of the filter, although some increase in spatial frequency has been noted for air samples by a great as 150% (15). Because the PAT round samples are created using a slower-moving fluid (such as water or toluene) as opposed to air (16, 17), less-significant differences in deposition frequency result from the flow regime having a much lower Reynolds number. Thus, the usual decline in fiber density along a radial path between the center of the filter and the perimeter of the filter is observed. The filters are rendered transparent (referred to as "cleared") by means of vaporized acetone (3, 18, 19) that dissolves and then redeposits a thin film containing the fibers onto a microscope slide. The cleared filter is then fixed with triacetin (3). The triacetin slides may last for several years but can degrade more rapidly than that (20-22). At the time, the samples that were analyzed in this study were less than four years old, although one sample filter (115-1) was newly mounted from a 13-year-old filter.

The development of fiber counting of airborne samples using PCM has developed over the years. PCM is performed at a nominal 400-450X magnification which allows the detection of fibers as thin as 0.43 µm diameter, depending on the fiber type. The industry standard NIOSH 7400 method does not detect all fibers because of the limitations of microscopy, so that the method is only an index of exposure (23, 24). A test slide has been developed to allow a check of proper alignment and phase detection in the microscope (19), together with an eyepiece graticule to standardize the counting field as a circle of 100 µm diameter (25), and rules have been formulated for the identification and enumeration of fibers (24). The general format of the test slide is shown in Figure 4. An analyst in combination with a microscope is required to be able to detect down to at most a 0.45 µm wide ridges that are intended to represent phase specimens. Photomicrographs for the third set of grooves (0.64 µm wide) using PCM and HMC are shown in Figures 5 and 6.

The setup also includes the use of a Walton-Beckett Graticule (Figure 7) along with examples of suspect fibers as presented in the NIOSH 7400 Method (24). The standard counting method is the NIOSH 7400 Method with the A counting rules (24), which is used for both the PAT rounds and for personal sample analysis per the Occupational Safety and Health Administration (OSHA) regulations (26). The key aspects of the A counting rules are:

- Count only fibers > 5 µm in length.
- Count only fibers with > 3:1 length-to-width (aspect) ratio.
- Count a minimum of 20 fields and a maximum of 100 fields.
- Stop counting fields after 100 fibers are counted.
- Count one fiber if it is completely inside the Walton Becket Graticule.
- Count half fiber if crosses graticule perimeter only once.
- Count zero if crosses graticule line more than once or if is outside the graticule.

The significant variability in the counting of asbestos fibers is well recognized (24, 27, 28) and is generally modeled using the Poisson distribution statis-

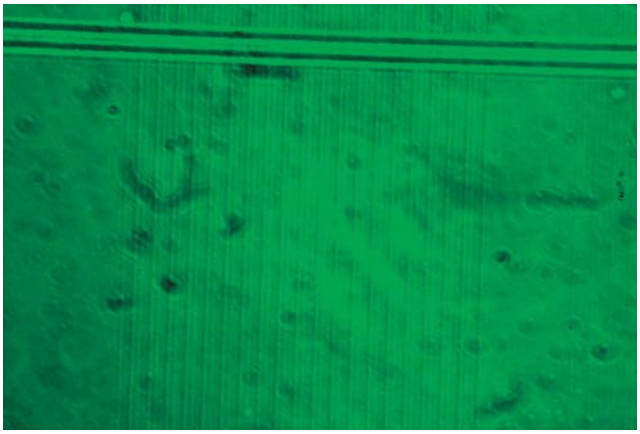

Figure 5. Photomicrograph of set 3 of the HSE/NPL test side using PCM. Ridge thickness of grooves is 0.64 µm.

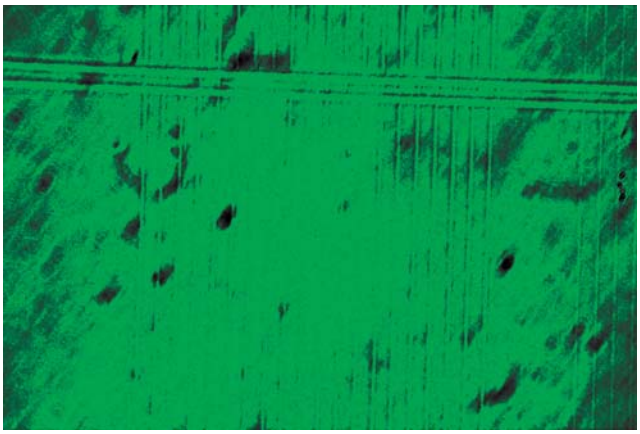

Figure 6. Photomicrograph of set 3 of the HSE/NPL test side using HCM. Ridge thickness of grooves is 0.64 µm.

tics (3). The variability in sample counting generally ranges from a minimum coefficient of variation (CV) of 0.10 to a high of 0.80, including interindividual variability revealed by CVs of as great as 0.40 (3, 27). Therefore, in order to determine differences with any modicum of statistical validity, the study was restricted to one analyst (the author) and a single microscope. The microscope used was a modified Olympus BH-2 using diffuse lighting. In the asbestos industry, PCM scopes almost exclusively use diffuse lighting as opposed to the more uniform Köhler illumination, the choice of illumination in this study. The microscope included a universal condenser to house all the optical elements for each technique (phase annulus for PCM, polarizing modulator for HMC and the prism for DIC).

In order to accommodate the DIC slider above the specimen and objectives, a turret with a 1.25X nominal magnification increase was necessarily added. This brought the overall magnification to 400X for both PCM and HMC, and 500X for DIC. The DIC magnification is slightly outside the NIOSH stated range of 400-450X (24). In accordance with the NIOSH 7400 A counting rules (24), a Walton Becket G-22 graticule was inserted into a 10X ocular for use in counting and field area determination. The standard graticule area for the PCM and HMC setups were 0.00785 mm^2 and 0.00503 mm^2 for DIC due to 1.25X slider magnification enhancement. Although graticule field area is recognized as a parameter that affects counting results (29), the difference between 80 and 100 mm diameter graticules is expected to be less than 10% and, therefore, insignificant in this study relative to other factors affecting visibility.

Objectives with nominal 40X magnification (phase or strain-free) were used with a numerical aperture (NA) of 0.65 for the phase objective and an NA of 0.70 for both HMC and DIC; the NIOSH 7400 method allows a range of 0.65-0.75 NA. The phase element in the objective and the phase annulus in the condenser were both circular (annular) in geometry for the PCM setup. A dichroic filter centered around a wavelength of 560 nm (green) was also used in all cases. The wavelength of 560 nm is recognized as being optimal for contrast detection under certain lighting conditions (30). The PCM technique applied positive phase contrast (black fibers on a light background) in accordance with the NIOSH 7400 method, although negative phase contrast (white fibers on a dark background) is recognized as superior for detection of particles (31).

EXPERIMENTAL DESIGN PART 2: DATA COLLECTION PROCESSING

Each of the samples was analyzed in random order once by PCM, HMC and DIC. The analyst was blind to the actual sample number but the morphologies of each are sufficiently distinct to allow determination of fiber type without foreknowledge. Asbestos fiber counts are recognized as following a Poisson distribution, and therefore, in order to normalize the fiber counts, the fiber density values were adjusted to make them more towards a normal distribution (12-13). The fiber density E in fibers per millimeter of filter area (f/mm^2) is define as:

$$E = \frac{(FCS/FLS) - (FCB/FLB)}{RFA} \qquad \text{Eq 1}$$

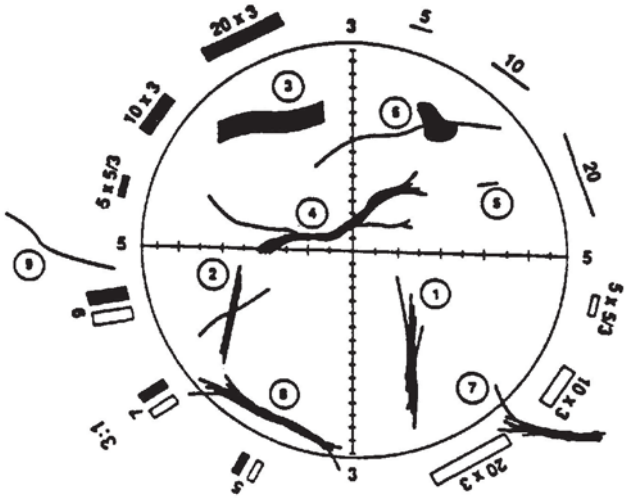

National Institute for Occupational Safety and Health

Figure 7. A Walton-Beckett Graticule with example fibers.

Where

E = Fiber Density (f/mm^2)
FCS = Fibers Counted in the Sample
FLS = Fields Counted in the Sample
FCB = Fibers Counted in the Blank
FLB = Fields Counted in the Blank

The data was transformed using

$$E' = (E)^{0.5} \qquad \text{Eq 2}$$

Where

E = Fiber Density (f/mm^2) from Equation 1
E′ = Transformed Fiber Density

In order to evaluate nominal differences between each of the techniques, PCM-HMC-DIC, the transformed fiber density values (E′) were compared to the NIOSH Reported PCM reference values as

$$\text{Ratio } (R_{PCM}) = \frac{E'_{PCM}}{E'_{Ref\ PCM}} \qquad \text{Eq 3}$$

$$\text{Ratio } (R_{HMC}) = \frac{E'_{HMC}}{E'_{Ref\ PCM}} \qquad \text{Eq 4}$$

$$\text{Ratio } (R_{DIC}) = \frac{E'_{DIC}}{E'_{Ref\ PCM}} \qquad \text{Eq 5}$$

In this way, normalized ratios were obtained to mean values ($E'_{Ref\ PCM}$) as reported by PCM for more than 1,200 laboratories. Ratios were also determined for HMC ($R_{HMC\text{-}PCM}$) and DIC ($R_{DIC\text{-}PCM}$) where ratios PCM analysis from the same analyst in data set were calculated using Equations 6 and 7.

$$\text{Ratio } (R_{HMC\text{-}PCM}) = \frac{E'_{HMC}}{E'_{PCM}} \qquad \text{Eq 6}$$

$$\text{Ratio } (R_{DIC\text{-}PCM}) = \frac{E'_{DIC}}{E'_{PCM}} \qquad \text{Eq 7}$$

Ratios relative to the standard deviation of the transformed PAT round PCM reference data were also calculated and reviewed for all three methods as represented by $R_{S\text{-}PCM}$, $R_{S\text{-}HMC}$ and $R_{S\text{-}DIC}$ per equations 8, 9 and 10, respectively. The NIOSH PAT round pass-fail criteria is based on whether a particular sample result is within plus or minus three standard deviations of the transformed mean (for all, 3S) (12). The results were compared also with this criteria. And finally, ratios were evaluated with respect to reported coefficients of variation (CVs) for each sample as determined from the NIOSH PAT round reference values reported and their respective one-, two- and three-standard deviation ranges.

$$\text{Ratio } (R_{S\text{-}PCM}) = \frac{E'_{PMC} - E'_{Ref\ PMC}}{S'_{Ref\ PCM}} \qquad \text{Eq 8}$$

Where $S'_{Ref\ PCM}$ = standard deviation of square root transformed data from PAT round.

$$\text{Ratio } (R_{S\text{-}HCM}) = \frac{E'_{HMC} - E'_{Ref\ PMC}}{S'_{Ref\ PCM}} \qquad \text{Eq 9}$$

$$\text{Ratio } (R_{S\text{-}DIC}) = \frac{E'_{DIC} - E'_{Ref\ PMC}}{S'_{Ref\ PCM}} \qquad \text{Eq 10}$$

RESULTS

The raw fiber density results are presented for chrysotile, amosite and MMMF samples in bar Graphs 1, 2 and **3**, respectively. The averages of each technique by fiber type are provided in Table 1. Fiber density ratios for each method compared to the reference PCM (R_{PCM}, R_{HMC}, R_{DIC}) are displayed in bar Graph 4 by fiber type (chrysotile, amosite and MMMF) along with error bars about the means. Fiber density ratios for HMC and DIC methods compared to the PCM ($R_{HMC\text{-}PCM}$, $R_{DIC\text{-}PCM}$) are displayed in bar Graph 5 by fiber

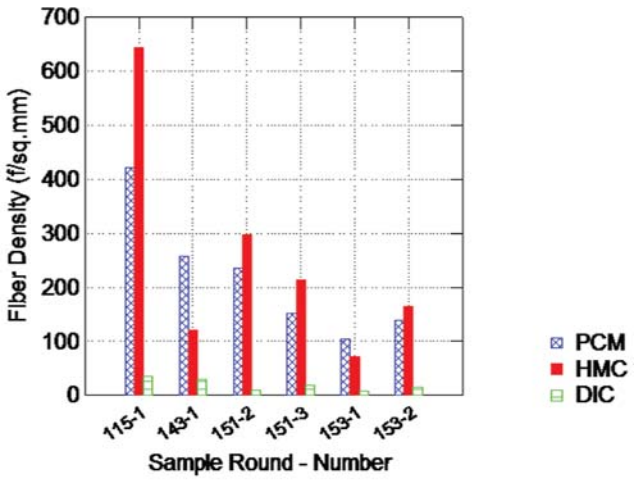

Graph 1. Raw fiber density of chrysotile samples by contrast method.

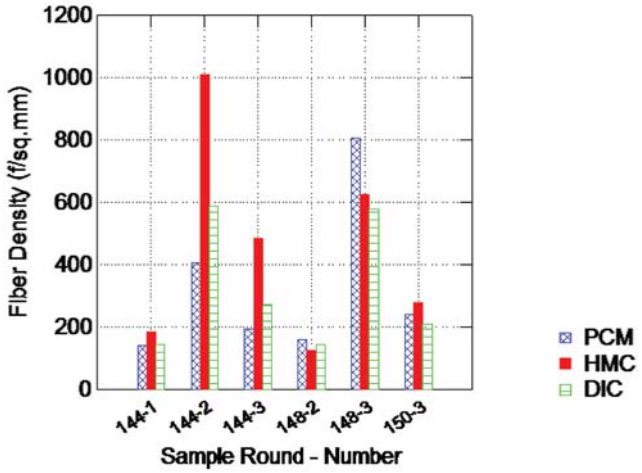

Graph 2. Raw fiber density of amosite samples by contrast method.

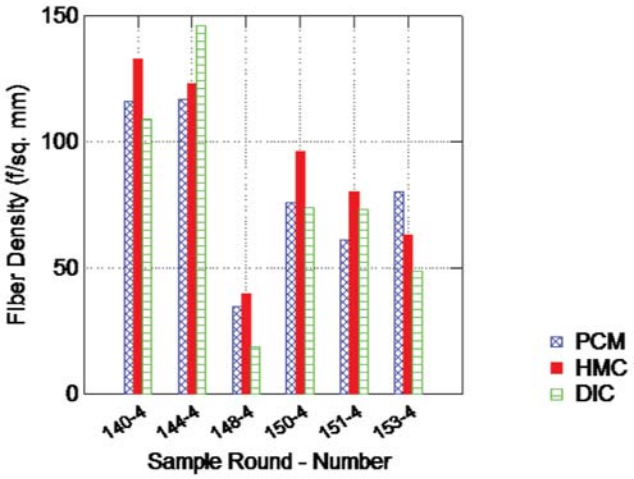

Graph 3. Raw fiber density of man-made mineral fiber (MMMF) samples by contrast method.

type (chrysotile, amosite and MMMF) along with error bars about the means. Ratios compared to the standard deviation from the reference samples are shown in Graph 6 by contrast and fiber type. Ratios compared to the coefficient of variation (CV) for the reference samples are shown in Graph 7 by contrast type.

Ratios compared to the standard deviation from the reference samples are shown in Graph 6 by contrast and fiber type. Ratios compared to the coefficient of variation (CV) for the reference samples are shown in Graph 7 by contrast type. Examples of DIC, HMC and PCM for amosite are provided as Figures 8-10 (note the slight scale difference for DIC). Examples of chrysotile are provided as Figures 11 and 12. A DIC example is not provided for chrysotile as the image quality was too poor to discern the chrysotile.

DISCUSSION

The first observation is that the analyst's PCM counts are consistently higher than the reference PCM values from the more than 1,200 laboratories. The author normally has fiber counts slightly above, to one standard deviation above, the reported mean reference value, and therefore this is expected in this case. The NIOSH 7400 method indicates an acceptable range of fiber densities in from 100-1,200 f/mm^2. Some of the MMMF are below this range, which is common for MMMF samples. The results do not appear to be affected by fiber type for MMMF, except that there is perhaps slightly lowered DIC results in the MMMF due to a smaller graticule field area. This results in fibers being more likely to cross over the graticule edges where they are counted as half a fiber instead of single fibers, therefore lowering the overall counts (29).

The graphic results reveal that the DIC results are significantly below both the referenced PCM values and the PCM count values for the chrysotile fiber and the MMMF samples by this one analyst. A standard t-test of paired counts for HMC paired to PCM, and DIC paired to PCM for all fiber types demonstrated no statistical significant differences between HMC and PCM ($p = 0.166$) but a significant difference between DIC and PCM ($p = 0.008$). Further analysis by fiber type indicated that the only statistically significant measure affecting the DIC to PCM ratio were the chrysotile fiber samples ($p < 0.005$). This difference is not completely unexpected can

Table 1. Raw Fiber Density Data Means by Contrast Technique and Fiber Type

Technique	Chrysotile (f/mm²)	Amosite (f/mm²)	MMMF (f/mm²)	All (f/mm²)
Phase Contrast (PCM)	325	218	81	208
Hoffman Modulation Contrast (HMC)	452	252	89	264
Nomarski Differential Contrast (DIC)	323	19	78	140
Mean of all	367	163	83	204

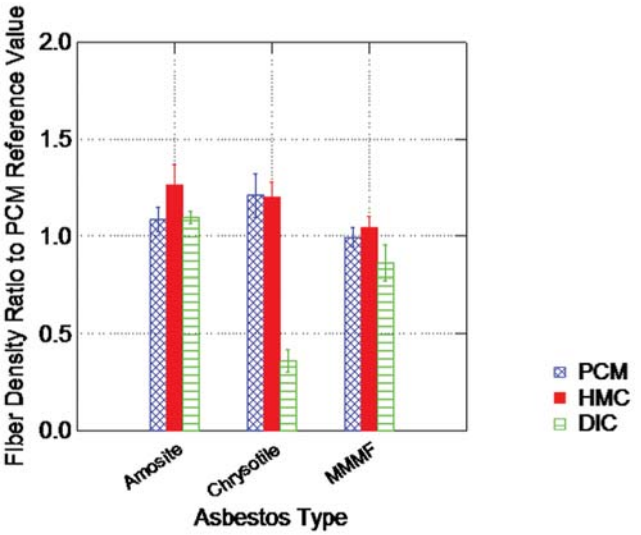

Graph 4. Ratio of transformed fiber density to the transformed referenced PAT round PCM values by contrast method and by fiber type.

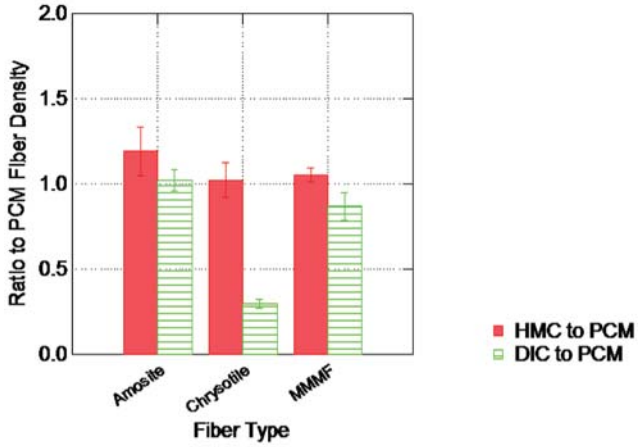

Graph 5. Ratio of transformed fiber density to the transformed PCM values from this study differentiated by contrast method and by fiber type.

be explained by looking at the optical aspects of the intensities of light transmitted through fibers in a sample and consequently the contrast differences.

It has been suggested that PCM is useful up to 1/2λ and best at <1/10λ, whereas DIC is useful from >1/10λ to 1λ and best above 1/2λ (32). Chrysotile asbestos has refractive indexes in the range of 1.53-1.56 (birefringent) and amosite in the range of 1.63-1.73 (birefringent) (33). MMMF depends upon the type, where mineral wool generally falls in 1.52-1.56 range (isotropic) but may be as high as 1.70, ceramic fibers are in the neighborhood 1.51-1.70 (isotropic), and fiber glass is in the range of 1.47-1.57+ (33). The maximum phase change through a fiber can be calculated using equation 11:

$$\varphi = |n_1 - n_2| t \qquad \text{Eq 11}$$

Where

φ = phase Change
n_1 = refractive index of medium at approximately 1.48 (NIOSH, 1994)
n_2 = refractive index of fiber
t = thickness of a fiber
λ = 560 nm (green light)

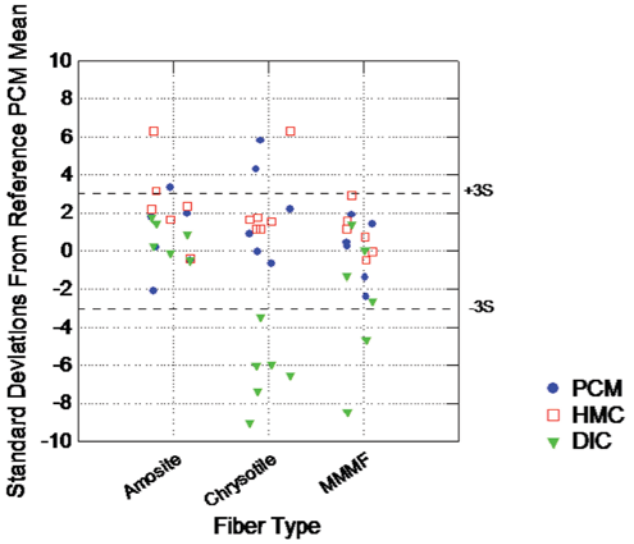

Graph 7. Ratio of transformed fiber density to the transformed referenced PAT round PCM values represented as fractions of the reference standard deviation of counts by PCM. Presented by contrast method and by fiber type.

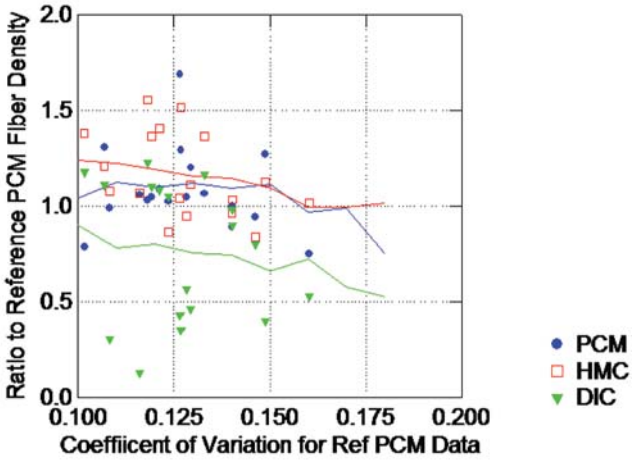

Graph 8. Coefficient of variation (CV) (data from more than 1,200 labs) versus the ratio of transformed fiber density to the transformed referenced PAT round PCM values. Presented by contrast method.

For chrysotile, one finds thin fibers at the limit of detection common in PAT rounds with a fiber diameter approximately 0.5 µm. Using 1.55 for the greatest difference in refractive index, results in a phase change on the order of 35 µm or 1/16 λ. For amosite, one finds thin fibers common in PAT rounds with a fiber diameter > 1 µm. Using the value 1.68 for the refractive index results in a phase change on the order of 200 µm or about 4/10 λ. For MMMF, the refractive index range varies considerably but the visibility of the fibers is primarily due to the much larger diameters, 5-40 µm in the case of most PAT rounds.

To evaluate the phase change effects as they relate to intensity, contrast, and subsequently the ability to distinguish fibers, one first must determine the relationship for each method in terms of intensity.

For PCM if one considers

$$\psi(x) = e^{i\chi(x)} \qquad \text{Eq 12}$$

Where

$$e^{i\varphi(x)} = 1 + i\varphi^1(x) - [\varphi^2(x)/2!] - [i\,\varphi^3(x)/3!]$$

For small changes

$$e^{i\varphi(x)} = 1 + i\varphi 1(x) \qquad \text{Eq 13}$$

$$\psi(u) = \int_{-\infty}^{\infty}\psi(x)\, e^{(-ikxu/f)}\, dx \text{ with } k = 2\pi \qquad \text{Eq 14}$$

$$\psi(u) = \psi_0 + \psi_1 \qquad \text{Eq 15}$$

Where $_0$ indicates the zero order frequency component.

For a phase change of p/2 then

$$\psi(x') = e^{i\pi/2} + e^{i\varphi(x')} - 1 \text{ (for the image plane)} \qquad \text{Eq 16}$$

The irradiance [I(x′)] is then determined from

$$I(x') = \psi(x')\,\psi^*(x') \qquad \text{Eq 17}$$

where * is the conjugate.

Therefore,

$$I(x') = 3 + 2\sin\varphi(x') - 2\cos\varphi(x') \qquad \text{Eq 18}$$

For small changes

$$I(x') = 1 - 2\varphi(x') \qquad \text{Eq 19}$$

And the gradient can be approximated as

$$\Delta I(x') = -2\varphi \qquad \text{Eq 20}$$

Therefore, the intensity changes linearly with phase change.

For HMC, Hoffman (8) has shown that

$$I(x') = T_g[P_A(x')]^2 + T_B[P_a(x')]^2 + T_G[P_A(x')]^2 -$$

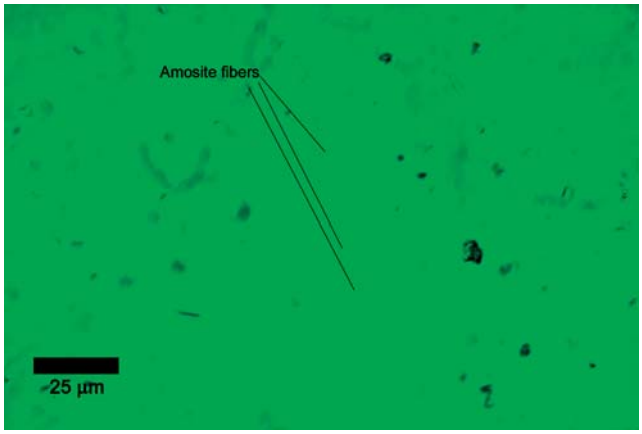

Figure 8. Example field with amosite fibers from Sample 148-1 by Nomarski DIC.

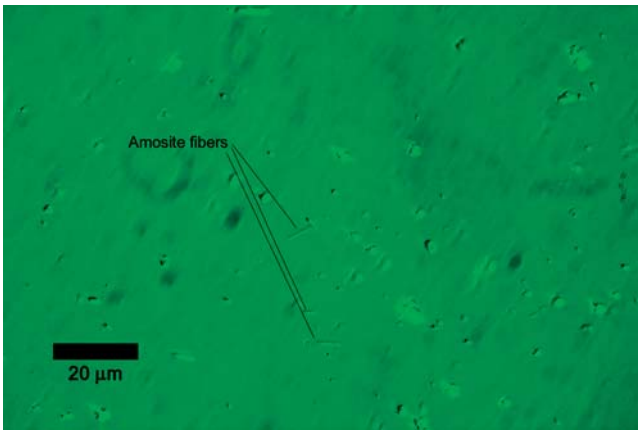

Figure 9. Example field with amosite fibers from Sample 148-1 by Hoffman Modulation Contrast.

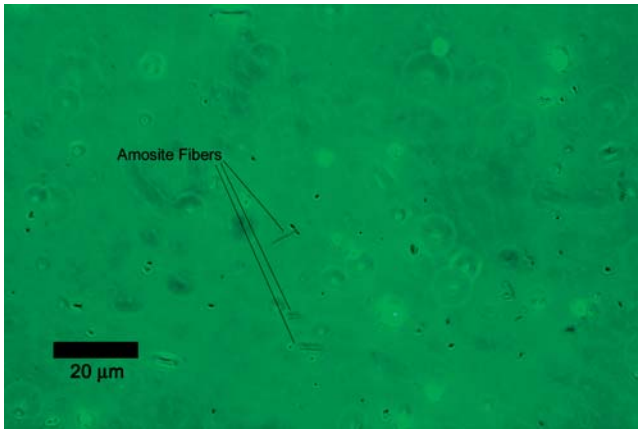

Figure 10.Example field with amosite fibers from Sample 148-1 by Phase Contrast Microscopy.

$$2T_G P_A(x')P_a(x') + 2(T_G T_B)^{1/2}P_A(x')P_a(x') \cos\varphi(x') - 2 (T_G T_B)^{1/2}[P_a(x')]^2\cos\varphi(x') \quad \text{Eq 21}$$

Where

T_B = Transmittance in bright region
T_G = Transmittance in gray region

Thus the change in intensity can be represented by

$$\Delta I = I_0 f \Delta\varphi(T_B - T_G)^2 \cos(\beta/w) \quad \text{Eq 22}$$

Where

f = focal length of the objective
w = width of slit
β = angle away from perpendicular slit

For DIC, one can consider two light rays mutually perpendicular as split when entering the Wollaston prism in the substage condenser:

$$\psi_1(x) = a_1 e^{i\theta(x)} \quad \text{Eq 23a}$$
$$\psi_2(x) = a_2 e^{i\theta(x)} \quad \text{Eq 23b}$$

Upon passing through a specimen at orthogonal positions, the light waves may be considered as:

$$\psi =_1(x) = a'_1 e^{i(\theta 1 - \varphi)(x)} \quad \text{Eq 24a}$$
$$\psi =_2(x) = a'_2 e^{i(\theta 2 - \varphi)(x)} \quad \text{Eq 24b}$$

Upon recombining and considering the intensity (I) result is

$$I(x) = a'^2_1 - a'^2_2 + 2a'_1 a'_2 \cos(\theta_1 - \theta_2 + 2\varphi) \quad \text{Eq 25}$$

Where

2φ is the bias of the prisms.

For almost pure phase objects with little or no amplitude absorption differences, equation 24 reduces to

$$I(x) = A Cos(\theta_1 - \theta_2 + 2\varphi) \quad \text{Eq 26}$$

Where

$$A = 2a'_1 a'_2$$

Thus the change in intensity can be represented by

$$\Delta I(x) = A Sin(\theta_1 - \theta_2 + 2\varphi) \quad \text{Eq 27}$$

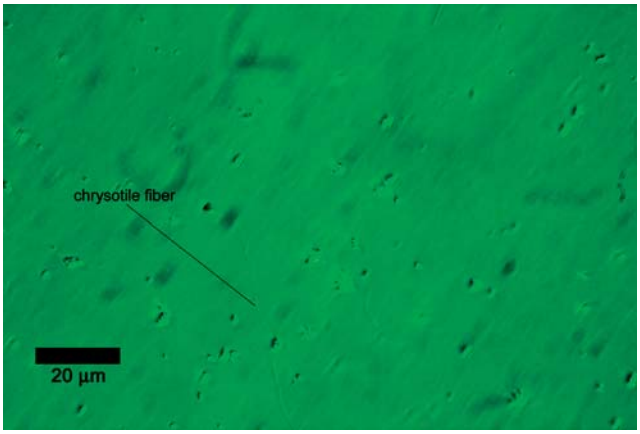

Figure 11. Example field with chrysotile fibers from Sample 151-3 by Hoffman Modulation Contrast.

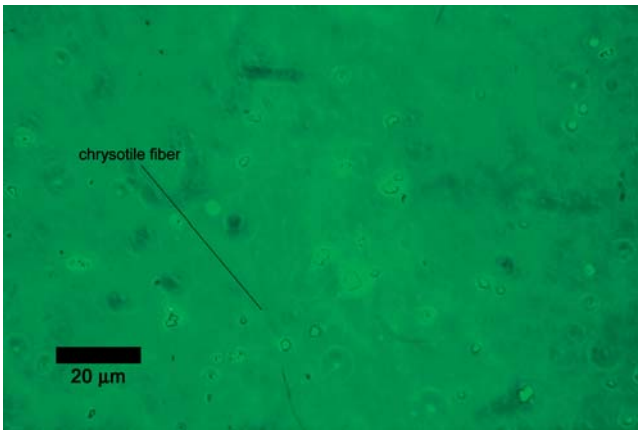

Figure 12. Example field with chrysotile fibers from Sample 151-3 by Phase Contrast Microscopy.

In summary, the techniques produce changes in intensity as follows:

PCM: $\Delta I(x') = -2\varphi$ Eq 20
HMC: $\Delta I = I_0 f \Delta\varphi (T_B - T_G)^2 \cos(\beta/w)$ Eq 22
DIC: $\Delta I(x) = A Sin(\theta_1 - \theta_2 + 2\varphi)$ Eq 27

Therefore, PCM provides contrast directly proportional to the phase of the object, HMC directly proportional to the gradient of the phase and DIC proportional to the sine of the phase. With typical bias ($\grave{e}_1 - \grave{e}_2$) in DIC, the contrast does not change appreciably compared to either PCM or HMC, therefore the inability to discern the thin chrysotile fibers that approach the shearing distance. The intensity change directly proportional to the phase provides the choppiness to PCM, whereas the intensity change in HMC is *smoothed* by being proportional to the gradient of the phase change.

CONCLUSIONS

It is clear from the photomicrographs and statistical evaluation of the counting data that Nomarski differential interference contrast performed satisfactorily for MMMF, poorly for amosite and very poorly for chrysotile. On the other hand, Hoffman modulation contrast performed comparable to phase contrast microscopy for MMMFs, amosite and chrysotile. Subjectively, Hoffman modulation contrast demonstrated less interference in the form of artifacts like halos and light scattering, and was also qualitatively less fatiguing than PCM. Therefore, HMC would be a suitable alternative to PCM for asbestos fiber counting; DIC would not.

ACKNOWLEDGMENTS

This article is dedicated to the late Dr. Paul Baron from whom many owe much about asbestos fiber counting and aerosol science.

REFERENCES

1. Edwards, G.H. and Lynch, J.R. "The Method Used by the U.S. Public Health Service For Enumeration of Asbestos Dust on Membrane Filters," *The Annals of Occupational Hygiene,* **11,** pp 1-6, 1968.

2. National Institute for Occupational Safety and Health (NIOSH). "Analytical Method P&CAM 239," *NIOSH Manual of Analytical Methods* (2nd edition), I. DHEW (NIOSH) Publication No. 77-157-A 239, 1977.

3. National Institute for Occupational Safety and Health (NIOSH). *Proficiency Analytical Testing Program & Environmental Lead Proficiency Analytical Testing Program (PAT & ELPAT) Programs*, NIOSH Pub. 95-104. U.S. DHHS: Cincinnati, November, 1994.

4. Baron, P.A., Sorense, C. and Brockmann, J.E. "Nonspherical Particle Measurements: Shape Factors, Fractals, and Fibers," *Aerosol Measurement: Principles, Techniques, and Applications* (2nd edition), edited by Paul A. Baron and Klause Willeke. John Wiley & Sons: New York, pp 705-749, 2001.

5. Chatfield, E.J. "Asbestos measurements in workplaces and atmospheres." *Electron Microscopy in Forensic, Occupational and Environmental Health Sciences,* Edited by S. Basu and J.R. Millette. Plenum Publishing: New York, pp 149-186, 1986.

6. Born, M. and Wolf, E. *Principles of Optics,* Pergamon Press: New York, 1959.

7. Ross, K.F.A. *Phase Contrast and Interference Microscopy,* St. Martin's Press: New York, 1967.

8. Hoffman, R. and Gross, L. "Modulation Contrast Microscope," *Applied Optics,* **14(5),** pp 1169-1176, 1975.

9. Hoffman, R. "The modulation contrast microscope: principles and performance," *Journal of Microscopy,* **110(3),** pp 205-222, 1977.

10. Hartley, W.G. "A Consideration of The Hoffman Modulation Contrast," *Journal of Microscopy,* **33,** pp 147-152, 1977.

11. Nomarski, G. and Weill, A.R. "Sur L'observation des figures de croissance des cristaux par les methodes interferentielles a deux ondes," *Bulletin de la Societe Francaise de Mineralogie et de Cristallographie,* **78,** pp 840-868, 1954.

12. National Institute for Occupational Safety and Health (NIOSH). *Laboratory Reports and Criteria for the Proficiency Analytical Testing Program (PAT),* NIOSH Pub 91-102. U.S. DHHS: Cincinnati, June, 1990.

13. Schlecht, P.C. and Shulman, S.A. "Performance of asbestos fiber counting laboratories in the NIOSH proficiency analytical testing (PAT) program," *American Industrial Hygiene Association Journal,* **47(5),** pp 259-269, 1986.

14. Schlecht, P.C. and Shulman, S.A. "Phase Contrast Microscopy Asbestos Fiber Counting Performance in the Proficiency Analytical Testing Program," *American Industrial Hygiene Association Journal,* **56(5),** pp 480 489, 1995.

15. Feigley, C.E., et. al. "Asbestos Fiber Deposition Patterns on Various 25-mm Cassette Filters at High Flow Rates," *Applied Occupational Hygiene,* **7(11),** pp. 749-757, 1992.

16. Teichman, J. and Parish, H. "Standard Reference Asbestos Samples for Optical Microscopy Quality Assurance Programs," *NAC Journal,* pp 33-38, Fall 1988.

17. Baron, P.A. and Deye, G.J. "Generation of Duplicate Asbestos Aerosol Samples for Quality Assurance," *Applied Industrial Hygiene,* **2(3)**, pp 114-118, 1987.

18. Baron, P.A. and Pickford, G.C. "An asbestos sample filter clearing procedure," *Applied Industrial Hygiene,* **1**, pp 169-171, 1986.

19. LeGuen, J.M.M., Ogden, T.L., Shenton-Taylor, T. and Verrill, J.F. "The HSE/NPL phase-contrast test slide," *The Annals of Occupational Hygiene,* **28,** pp 237-247, 1981.

20. Pang, T.W.S. "Precision and accuracy of asbestos fiber counting by phase contrast microscopy," *American Industrial Hygiene Association Journal,* **61,** pp 529-538, 2000.

21. Schenton-Taylor, T. and Ogden, T.L. "Permanence of Membrane Filter Clearing and Mounting Methods for Asbestos Measurement," *The Microscope,* **34(3),** pp 161-172, 1986.

22. Ogden, T.L. and Thompson, D.J.M. "Euparal and Its Use in Measurement of Asbestos," *The Microscope,* **34(3),** pp 173-179, 1986.

23. Baron, P.A. "Measurement of airborne fibers: A review," *Industrial Health,* **39,** pp 39-50, 2001.

24. National Institute for Occupational Safety and Health (NIOSH). Fibers, method 7400 issue #2 (8/15/94). In *NIOSH Manual of Analytical Methods* (4th edition), Pub. 94-113, NIOSH: Cincinnati, 1994.

25. Walton, W.H. and Beckett, S.T. "A microscope eyepiece graticule for the evaluation of fibrous dusts," *The Annals of Occupational Hygiene,* **20,** pp 19-23, 1977.

26. Occupational Safety and Health Administration. "*29 CFR 1926.11001, Appendix A to 1926.1101 - OSHA Reference Method (Mandatory),*" U.S. GPO: Washington D.C., 2008.

27. Ogden, et. al. "Within-Laboratory Quality Control of Asbestos Counting," *The Annals of Occupational Hygiene,* **30,** pp 411-425, 1986.

28. Occupational Safety and Health Administration. "*29 CFR 1926.11001, Appendix B to 1926.1101 - Sampling and Analysis (Non-Mandatory),*" U.S. GPO, Washington D.C., 2008.

29. Cherrie, J.W. "The Effect of Microscope Graticule Size and Counting Rules on the Estimation of Airborne Fibre Numbers Using the Membrane Filter Technique," *The Annals of Occupational Hygiene,* **28(2),** pp 229-236, 1984.

30. Bouma, P.J. *Physical Aspects of Colour*, NV Philips Gloeilampenfabrieken: Netherlands, p 39, 1947 (translation of Dutch text).

31. Rooker, S.J., Vaughn, N.P. and LeGuen, J. "On the visibility of fibers by phase contrast microscopy," *American Industrial Hygiene Association Journal,* **43(7),** pp 505-515, 1982.

32. McCrone, W.C., McCrone, L. and Delly, J. *Polarized Light Microscopy,* McCrone Research Institute: Chicago, 1984.

33. McCrone, W.C. *Asbestos Identification,* McCrone Research Institute: Chicago, 1987.